Chemistry Europe
European Chemical Societies Publishing

WILEY VCH

Excellence in Chemistry Research

Announcing our new flagship journal

- Gold Open Access
- Publishing charges waived
- Preprints welcome
- Edited by active scientists

Meet the Editors of *ChemistryEurope*

Luisa De Cola
Università degli Studi di Milano Statale, Italy

Ive Hermans
University of Wisconsin-Madison, USA

Ken Tanaka
Tokyo Institute of Technology, Japan

ChemPlusChem

A Multidisciplinary Journal Centering on Chemistry

Chemistry Europe

European Chemical Societies Publishing

Accepted Article

Title: In Situ DRIFTS Analysis during Hydrogenation of 1-Pentyne and Olefin Purification with Ag Nano Particles

Authors: Misael Cordoba Arroyo, Lina Garcia, Juan Badano, Carolina Betti, Fernando Coloma-Pascual, Monica Esther Quiroga, and Cecilia Lederhos

To be cited as: *ChemPlusChem* **2023**, e202300344

Link to VoR: https://doi.org/10.1002/cplu.202300344

WILEY VCH

WILEY-VCH

RESEARCH ARTICLE

In Situ DRIFTS Analysis during Hydrogenation of 1-Pentyne and Olefin Purification with Ag Nano Particles

Misael Cordoba,[a,b] Lina Garcia,[a,c] Juan Badano,[a] Carolina Betti,[a] Fernando Coloma-Pascual,[d] Mónica Quiroga, *[a] and Cecilia Lederhos,[a]

[a] Dr. M. Cordoba, Dra. L. Garcia, Dr. J. Badano, Dra. C. Betti, Prof. M. Quiroga, Dra. C. Lederhos
Instituto de Investigaciones en Catálisis y Petroquímica (INCAPE)
Colectora Ruta Nacional 168 Km 0 (Santa Fe, Argentina)
E-mail: mquiroga@fiq.unl.edu.ar
[b] Dr. M. Cordoba
Grupo de Investigación en Catálisis, Universidad del Cauca
Calle 5 No. 4-70 (Popayán, Colombia)
[c] Dra. L. Garcia
Grupo de Investigación Ciencia e Ingeniería en Sistemas Ambientales (GCISA), Universidad del Cauca
Calle 5 No. 4-70 (Popayán, Colombia)
[d] Dr. F. Coloma Pascual
Servicios Técnicos de Investigación, Universidad de Alicante,
Apartado 99 (Alicante, España)

Abstract: The catalytic performance of nanoparticles (NPs) of Ag anchored on different supports was evaluated during the selective hydrogenation of 1-pentyne and the purification of a mixture of 1-pentene/1-pentyne (70/30 vol %). The catalysts were identified: Ag/Al (Ag supported on ɣ-Al_2O_3), Ag/Al-Mg (Ag supported on ɣ-Al_2O_3 modified with Mg), Ag/Ca (Ag supported on $CaCO_3$) and Ag/RX3 (Ag supported on activated carbon-type: RX3). Besides, *in situ* DRIFTS analysis of 1-pentyne adsorption on each supports, catalysts and 1-pentyne hydrogenation were investigated. The results showed that the synthesized catalysts were active and very selective (≥85%) for obtaining the desired product (1-pentene). Different adsorbed species (-C≡C- and -C=C-) were observed on the supports and catalysts surface using *in situ* DRIFT analysis, which can be correlated to the activity and high selectivity reached. The role of the supports and electronic properties over Ag improve to H_2 dissociative chemisorption during the hydrogenation reactions; promoting the selectivity and the high catalytic performance. Ag/Al and Ag/Al-Mg were the most active catalysts. This was due to the synergism between the active Ag^0/Ag^+ species and the supports (electronic effects). The results show that Ag/Al and Ag/Al-Mg catalysts have favorable properties and are promising for the alkyne hydrogenation and olefin purification reactions.

Introduction

Selective hydrogenation reactions have been widely studied for many years on a global scale due to their scientific and industrial importance since they allow the valorization of products for different processes [1-3]. An interesting example is the hydrogenation reaction of unsaturated compounds, both alkenes and alkynes are of interest because their products are used in the pharmaceutical, food, agricultural, and fine chemical industries, among others. The catalytic hydrogenation of alkynes is one of the methods that allows obtaining alkenes [2, 3]. The great challenge when hydrogenating these molecules is to stop at a specific intermediate point, before reaching full hydrogenation to the alkane (saturated product). A crucial and much more applied stage in the industry is the selective transformation of alkynes in raw material streams as alkenes or the selective hydrogenation of triple bonds (C≡C) present in molecules with the presence of functional groups susceptible to hydrogenation such as: C=C, C=O, among others [4-6]. Specific examples of these processes are the selective hydrogenation of acetylene (HC≡CH) in a current rich in ethylene ($H_2C=CH_2$) in the hydrorefining of hydrocarbons and, similarly, the semi-hydrogenation of a vitamin A intermediate, where the present triple bond is partially hydrogenated forming a tetraene [7-10].

There is a great diversity of catalysts for selective hydrogenation, since it is one of the most versatile organic synthesis routes. The most widely used heterogeneous catalysts are noble metals, such as Pt, Pd, Ru, Rh, which generally have higher activity and selectivity, but their cost is high [1, 11]. On the other hand, other elements such as Ni, Ag, W, Cu, Fe, Cr, Co and their oxides can be used, as they are active and cheaper [5, 12-17].

Silver has a low affinity towards hydrogen due to the filled *d*-band (d^{10}), as opposed to metals such as nickel, palladium, and platinum (d^8) [18, 19]. Thus, the weak interaction of hydrogen with its extended metal surfaces such as found in single crystals and polycrystalline surfaces provides minimal dissociative chemisorption [20]. This inhibits the production of unwanted over-hydrogenated products due to limited surface saturation by hydrogen. Several supports have been tried to improve the catalytic properties of Ag based catalysts [13, 18, 20-23].

The kind of support can improve or decrease the activity/selectivity of the catalysts [24, 25]. In fact, the chemical and electronic properties generated due to metallic sites and support interactions, improves the catalyst performance [26]. While its structural properties affect the diffusion and adsorption of reagents and desorption of generated products [7]. To optimize the performance of catalysts, it is essential to understand the effect of the support on the catalytic activity during the selective hydrogenation reaction [27].

On the other hand, in the last decade Diffuse Reflectance Infrared Fourier Transform Spectroscopy (DRIFTS) has become a very popular method for the characterization of catalysts and it has been applied quite extensively to the identification of all adsorbed species on the surface, and consequently can contribute to the identification of reaction intermediates [28]. Recent works of catalytic systems using infrared spectroscopy to study the adsorption of alkynes and alkenes over supported metal catalysts and single crystals, have been published [14, 16, 29-34].

There are very few researches over the use of heterogeneous Ag catalysts during the selective hydrogenation of pure alkynes at mild operational conditions, neither regarded the purification or alkene/alkyne mixtures. Besides, to optimize the performance of Ag catalysts, it is essential to understand the effect of the support over the catalytic activity during the selective hydrogenation processes.

In previous works of our group, during the selective hydrogenation of alkynes and the purification of alkyne/alkene mixtures with Pd catalysts, it was found that the use the different supports had

electronic and geometric effects that improved the activity of Pd catalysts [7, 11, 29]. However, the effect of the acidity, surface properties and intermediate species over Ag catalysts with different supports has not been investigated in detail for selective hydrogenation of medium/long chain alkynes neither for the purification of alkene/alkyne mixtures.

The objectives of this work are: a) To synthesize and characterize Ag NPs catalysts using different supports: γ-Al_2O_3, γ-Al_2O_3 modified with Mg, $CaCO_3$ and an activated carbon; b) To monitor the adsorption and hydrogenation of pure 1-pentyne by means of in situ DRIFTS; and c) To evaluate the activity and selectivity of supported Ag NPs catalysts during the purification of 1-pentene in an alkyne/alkene (1-pentyne/1-pentene) stream and during the 1-pentyne (C_5) hydrogenation at mild operational conditions.

Results and Discussion

Catalysts Characterization

Table 1. Ag loadings, average particle sizes (d_{XRD} , d_{TEM}) by XRD and TEM results and dispersions (D_{TEM}).

Sample	ICP Ag (wt %)	d_{XRD} (nm)	d_{TEM} (nm)	D_{TEM} (%)
Ag/Al	0.54	2.4	2.9	40.6
Ag/AlMg [a]	0.58	3.6	3.2	36.8
Ag/Ca	0.42	17.6	19.4	6.1
Ag/RX3	0.40	17.7	11.6	10.2

[a] Mg: ICP: 2.5%

Table 1 shows the Ag loadings measured by ICP, average particle crystallite sizes (d_{XRD}) determined by XRD and average particle sizes (d_{TEM}) and dispersions (D_{TEM}) obtained from HRTEM microscopy. The synthetized catalyst has an Ag content between 0.40 and 0.58 wt% similar to the theoretical values. Furthermore, a metal loading of 2.5 wt % of Mg was detected in Ag/Al–Mg.

Figure 1 and **Figure 2S** (Electronic Supporting Information: SI) shows the HRTEM images, electron diffraction patterns and particle size distribution of the catalysts, respectively. It allowed calculating the d-spacing ~ 0.24 nm, which is characteristic of the Ag (111) on the catalytic surface [35]. Besides, the average particle size values for catalysts were estimated by XRD, d_{XRD}, and HRTEM, d_{TEM} and informed in **Table 1**. For the calculation of d_{XRD}, the Debye-Scherrer correlation and the deconvolution peak of Ag around 2θº: 37-39 were used (SI: **Equation 1, Figure 1S** and **Table 1S**). While **Equations 2** and **3** of SI, allowed to calculate the TEM particle diameter (d_{TEM}) and the metallic dispersion (D_{TEM}). Both techniques confirmed the presence of nanoparticles of Ag between 2.4-19 nm by XRD or HRTEM. Ag/Al, Ag/AlMg and Ag/Ca catalysts show similar values in both analyses (relative error ca. 10-15%), while the Ag/RX3 catalysts has a smaller average particle size by HRTEM. The order of particle size increases as follows: Ag/Al < Ag/Al-Mg <<< Ag/RX3 ≤Ag/Ca. From these results, considering the spherical particle model [35] and using ρ_{Ag}= 10.49 10^6 g_{Ag} m^{-3}; σ_{Ag} = 1.15 10^{19} at_{Ag} m^{-2} (**Table 2S**) the metal dispersions (D_{TEM}) were calculated and presented in **Table 1**. In Ag/Al and Ag/AlMg high percentages of dispersion were observed (~ 40-37%), while for the Ag/RX3 and Ag/Ca catalysts an intermediate and the lowest dispersion were obtained, respectively.

As observed in the results on Al_2O_3 and Al_2O_3-Mg supports, the highest values of metal content and smaller particle size were obtained, indicating that the Ag^+ species of precursor interacts more efficiently with the Al_2O_3 supports.

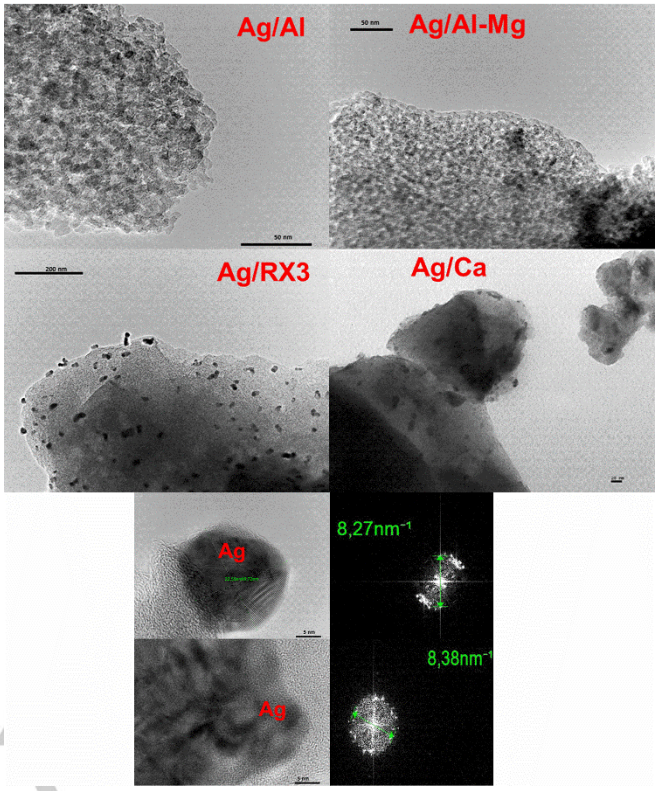

Figure 1. TEM analysis and electron diffraction patterns of catalysts.

As reported in a previous works of our group [7, 11], Al_2O_3, Al_2O_3-Mg and $CaCO_3$ supports showed by Temperature Programed Desorption of Pyridine (TPD-Py) different total acidity 32.6, 63.6 and 1.0 μmol_{Py} g^{-1}, respectively. According to Pyridine DRIFT and TPD, γ-Al_2O_3 support had acid sites, mainly Brönsted acidic sites. Besides, Al_2O_3-Mg support had the highest Lewis acidic strength and $CaCO_3$ support exhibited the lowest or null acidity. While the Pyridine DRIFT analysis showed that activated carbon RX3 presents both Brönsted and Lewis acid sites, due to the presence of different surface functional groups that could be responsible for the interaction with the precursor metallic salt [7]. Besides, the Ag loadings and average particle sizes results could be related to differences in BET pore volumes (V_p) and pore diameter (d_p) of supports. As reported in a previous work [7, 11] Al_2O_3, Al_2O_3-Mg, $CaCO_3$ and RX3 supports showed a S_{BET} of 180, 120, 4, 1,524 m^2 g^{-1}; a V_p of 0.53, 0.22, 0.01, 0.62 cm^3 g^{-1}; and a d_p 9.6, 7.2, 10.6, 26.7 nm, respectively. Higher particle sizes and low dispersion of Ag/$CaCO_3$ catalyst can be attributed to a low area and acidity of the support, thus promoting a greater agglomeration of the particles in the pore mouths. The intermediate particle size and dispersion of Ag/RX3 catalyst estimated by TEM images, can be attributed to the presence of the high amount of super micro and micro pores of this carbonaceous support (shape effects), and to the presence of surface groups (electronic effects), both factors promote the agglomeration of silver particles.

Figure 2 shows the XPS spectra of the Ag $3d_{5/2}$ and $3d_{3/2}$ regions of catalysts pretreated in hydrogen at 673 K, both regions are separated by approximately 6 eV, in total accordance with literature [36, 37]. The points are the experimental data and the curves beneath are the corresponding deconvoluted peaks. XPS results Ag $3d_{5/2}$ peaks and atomic ratios of Ag/X (where X=Al for alumina based catalysts, X=Ca for $CaCO_3$, or X=C for carbon

based material), for the Ag/Al, Ag/Al–Mg, Ag/Ca and Ag/RX3 catalysts These results are detailed in **Table 2**, two BE peaks for Ag/Al and Ag/Al-Mg catalysts at 368.2 ± 0.3 eV and 369.5 ± 0,25 eV, respectively which are assigned to Ag°/Ag^{+} and Ag^{+}-Al_2O_3 [38, 39]. Ag/Ca and Ag/RX3 catalysts present a BE peak for Ag $3d_{5/2}$ at 368.1 and 368.3 eV (100 $^{at}/_{at}$ %), respectively, indicating the presence of Ag^0/Ag^+ [36]. In the case of Ag^0/Ag^+ species found over the synthesized catalysts surface, a specific species can not be assigned due to possibility of the Ag^0 species to oxidize even under vacuum conditions. As reported by Ferreira et al. [39] the assignment of Ag oxidation state by XPS is a subject of great controversy. In fact, in the literature there is a great deal of disagreement for the assignment of binding energy values of the most intense peak: Ag $3d_{5/2}$. In Ag/Al–Mg the BE of the Mg 1s signal was located at 1304.9 eV and it was attributed to MgO surface species [7, 36].

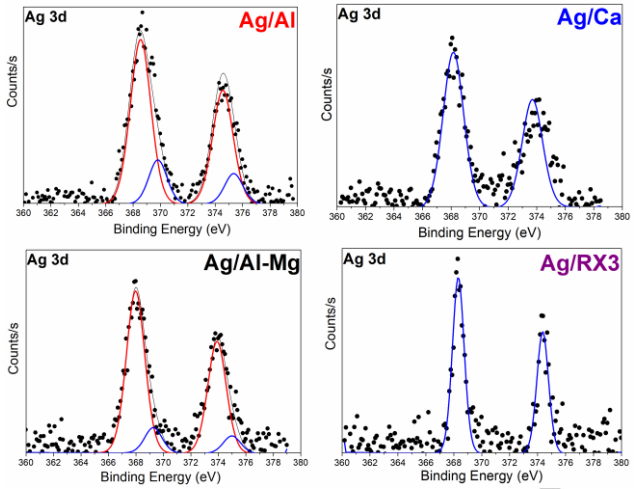

Figure 2. XPS spectra of the Ag 3d region of all catalysts

Table 2. XPS results of catalysts

Sample	XPS Ag $3d_{5/2}$ BE (eV)			
	△BE (eV)	Ag°/Ag^{+}	Ag^{+}-Al_2O_3	Ag/X[a] ($^{at}/_{at}$ %)
Ag/Al	6.1	368.5 (86%)	369.8 (14%)	0.0059
Ag/AlMg[b]	5.9	367.9 (87%)	369.3 (13%)	0.0099
Ag/Ca	5.5	368.1 (100%)		0.0138
Ag/RX3	6.1	368.3 (100%)		0.0017

[a] Ag/X: superficial atomic ratio, where X=Al for Ag on Al_2O_3 and Al_2O_3-Mg; X=Ca for Ag on $CaCO_3$ and X=C for Ag on RX3.
[b] Mg: XPS=1s: 1304.9 eV

Values of the superficial Ag/X (X = Al for Al_2O_3 and Al_2O_3-Mg; Ca for $CaCO_3$ and C for RX3) ($^{at}/_{at}$ %) atomic ratios are also shown in **Table 2**. For Ag/Ca catalyst the Ag/Ca atomic ratio was the highest (0.0138). The Ag/Al ratio is ca. 1.7 times higher for Ag/Al–Mg in comparison to Ag/Al, while for Ag/RX3 the Ag/C atomic ratio was the lowest (0.0017). Low values of BET area, pore volume and pore diameter on support favor a high content of Ag at a surface level.

Figure 3 shows the XRD diffractograms of the catalysts and their corresponding database references (Ag, $CaCO_3$, Al_2O_3 and RX3). For the Ag/Al–Mg and Ag/Al_2O_3 samples the presence of γ-alumina characteristic peaks at maximum intensity 2θ=37.7°, 45.9° and 66.9° are seen. Ag/Ca presents the characteristic peaks of the calcium carbonate at 2θ= 22.9°, 29.4°, 35.8°, 39.4°, 43.0°, 47.3°, 48.4°, 57.4°, 60.8°, 64,8°. Ag/RX3 has characteristic peaks of graphitic carbon at 2θ = 27° and 45°[7, 11].

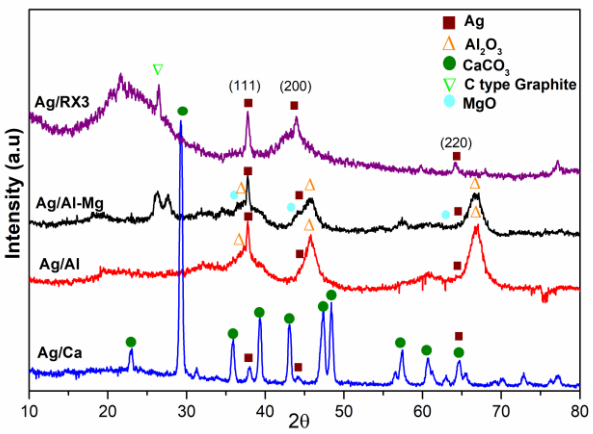

Figure 3. XRD diffractograms of the catalysts.

On the catalysts, the characteristic peaks of metallic Ag at 2θ = 38.1°, 44.3° and 64.5° corresponding to planes (111), (200) and (220), respectively, are observed in different proportions [40, 41]. When comparing the patterns found with those reported in the bibliography and HRTEM analysis, it could be estimated that the typical Ag pattern synthesized has an FCC structure [42]. Besides, over Ag/Al-Mg sample, very low intensity peaks were detected at 2θ = 36.9°, 42.8° and 62.2° which correspond to MgO. From the data obtained by XRD.

In situ DRIFTS Investigations

The *in situ* DRIFTS adsorptions of 1-pentyne and its hydrogenation analysis allowed to identify some adsorbed species and the chemical properties exhibited by the supports and the catalysts. The adsorption of 1-pentyne on supports was initially studied, because it is essential to understand the effect of the support on the catalytic activity during the selective hydrogenation reaction and the metal-support interactions (MSI) over supported nanoparticles of Ag.

Figure 4 shows the DRIFTS spectra of 1-Pentyne adsorbed on Al_2O_3 (Al), Al_2O_3-Mg (AlMg), $CaCO_3$ (Ca) and RX3 supports at different adsorption times (left) and comparative at 30 min (right). The DRIFTS peaks of alkyne on the support surface show significant characteristic vibrations of adsorbed 1-Pentyne that increase with the contact time. The main peaks are associated to : vibration of ν(-C≡C-) at 2130-2120 cm^{-1}, the alkynyl bond of ν(H-C≡) at 3330-3320 cm^{-1} and 1500-1200 cm^{-1}, vibrations of CH_3 and CH_2 groups of the aliphatic chain ν(C-H) at 3000-2800 cm^{-1} and ν(-C≡CH) out-of-plane vibration at 650-640cm^{-1} [43-45].

In **Figure 4** (right) the adsorption studies over each support show changes on the of 1-Pentyne adsorbed DRIFTS spectra at 30 min of adsorption time. A negative signal of –OH groups of alumina at 3730 cm^{-1} is evidenced on Al and AlMg supports, which is attributed to the formation of hydrogen bonds with 1-pentyne with OH groups [32, 46, 47]. Furthermore, a signal at 3940 cm^{-1} is observed on Al, AlMg and Ca supports with different intensity, associated to the formation of a complex between OH groups and 1-Pentyne due to the dissociative adsorption; which are consistent with previous studies [29]. In **Figure 6** are schematically represented the species of 1-Pentyne adsorbed over Al **(1-3)**, AlMg **(1-4)** and Ca **(5)** supports [32, 46].

10.1002/cplu.202300344

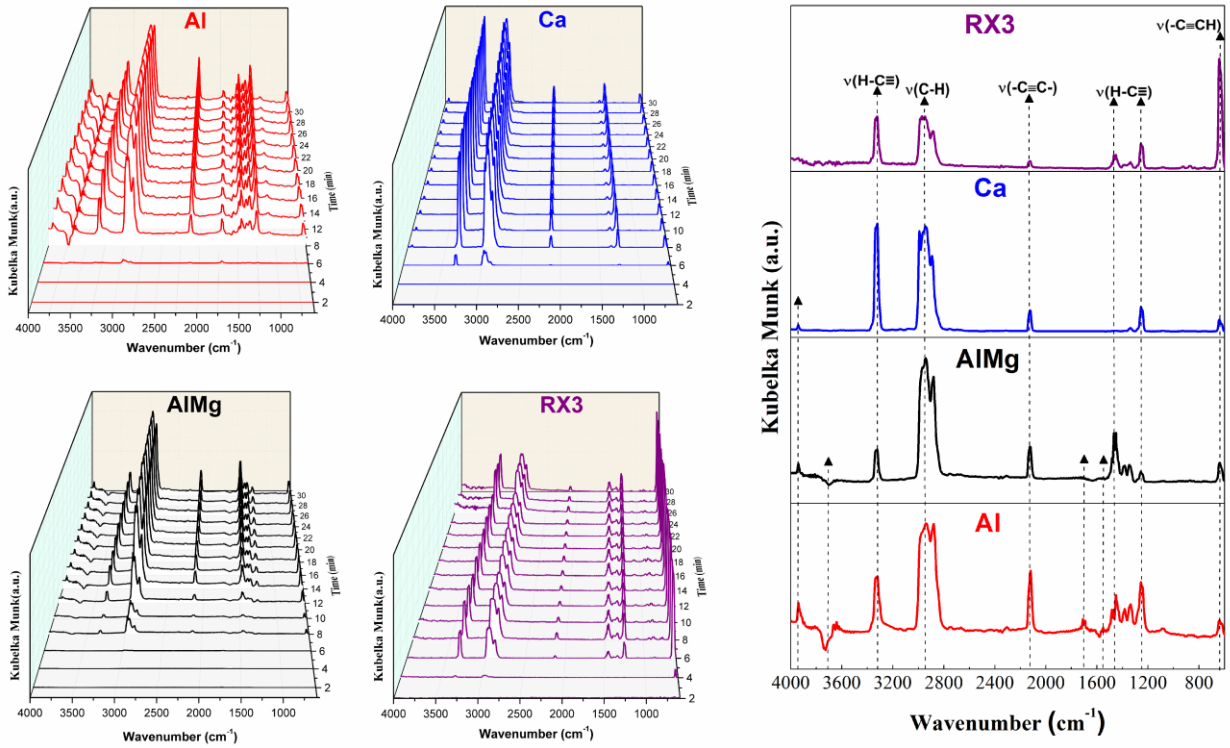

Figure 4. In situ DRIFTS analysis of supports at different 1-Pentyne adsorption time (left) and comparative at 30 min (right).

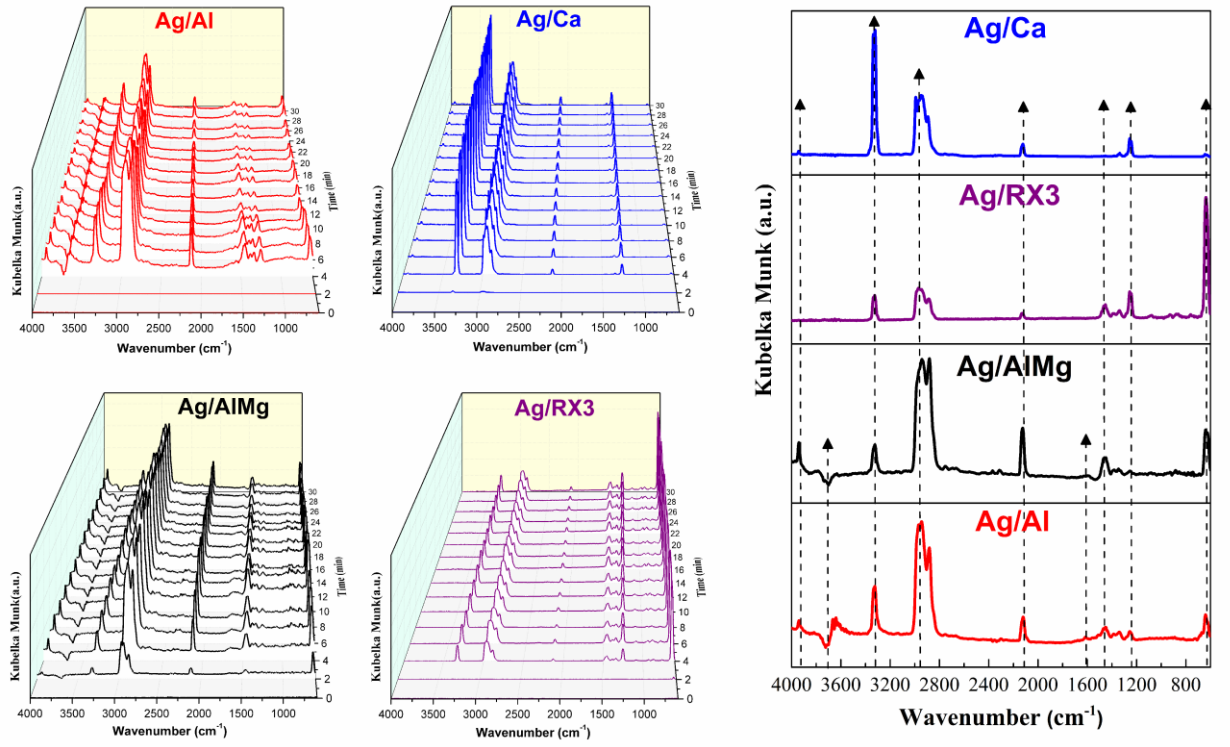

Figure 5. In situ DRIFTS analysis of catalysts at different 1-Pentyne adsorption time (left) and comparative at 30 min (right).

On the other hand, intermediate 1-Pentyne di-σ bond species ν(-C=C-) at ~ 1650 cm^{-1} and di-π adsorbed species between 1500 and 1200 cm^{-1} are observed on the surface of Al_2O_3 based supports [29, 30, 33, 47].

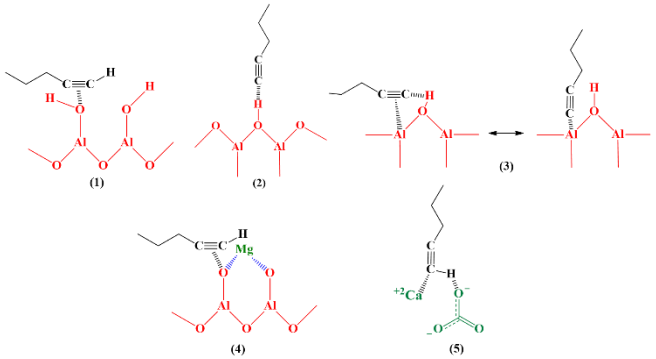

Figure 6. Schematic representations of 1-Pentyne adsorbed over the surface of Al, AlMg and Ca supports.

Further, in **Figure 4**, at 30 min of adsorption of 1-Pentyne are observed over the supports surfaces, changes in the intensity ratio of peaks ν_a (~1500 cm^{-1}) /ν_b (~1200 cm^{-1}), and also in the intensity vibration bands of the alkynyl bond ν (H-C≡) at 3330 cm^{-1} and ν(-C≡CH) out-of-plane vibration at 650 cm^{-1}. Ca, Al and RX3 supports present high intensity band at ~1250 cm^{-1}, while on AlMg support the peak at ~1465 cm^{-1} is more intense. The spectra also show the highest intensity peaks of ν(H-C≡) at 3300 cm^{-1} for Ca, and of ν(-C≡CH) at 685 cm^{-1} for RX3. These changes observed on *in situ* DRIFTS studies can be attributed to superficial differences of support properties causing different interactions between 1-Pentyne and the surface of each support [48]. The differences in the surface properties of the supports generate different interactions between the catalysts surface and the adsorbed alkyne, therefore modifying the IR bands intensities, especially those related to the ν (H-C≡) bond at 3320 and 1250 cm^{-1}. For $CaCO_3$ the high band observed at 3337 cm^{-1} of ν(H-C≡) is attributed to the basic character of the support. On the one hand, Ca^{2+}, a hard Lewis acid, interacts mainly with the π electrons of the alkyne (hard Lewis base) through di-σ bond species ν(-C=C-), and due to this, its H-C≡ hydrogen bond is remarkably acidic, due to the high *s* characteristic of the *sp* H-C bond, and can vibrate more intensively. On the other hand, intermediate 1-pentyne di-σ bond species ν(-C=C-) and di-π adsorbed species could change the intensity of the peak at ~1250 cm^{-1} due to the formation of these species modifying the vibration of alkynyl bond ν(H-C≡). Although, the incipient formation of green-oil adsorbed species could not be discarded, especially over the more acidic catalysts. These results could suggest the possible role of the support on the catalytic activity during the selective hydrogenation reaction and olefin purification.

Figure 5 shows the DRIFTS spectra of 1-Pentyne adsorbed on the Ag catalysts at different adsorption times (left) and comparative at 30 min (right). As previously discussed, similar vibration peaks of alkyne absorbed species over the catalysts surface are observed with different intensities respect with the supports. In the region of di-π adsorbed species (1500 - 1200 cm^{-1}), the DRIFTS spectra show analogous peaks compared with the supports. Besides, it is observed that Ag/Al has the most intense band at ~1450 cm^{-1} respect to the support peak. This can be attributed to different electronic superficial species of Ag. The bands in this region suggest that several species are formed by the partial break of the di-π ν(-C≡C-) bond of the adsorbed 1-Pentyne. This could be attributed to partial H- transfer of the residual H- species over Ag species and the interaction between the adsorbed alkyne with the surface groups in the supports. Furthermore, in **Figure 6,** the vibrations of intermediate species of -OH group between 3950-3600 cm^{-1}, ν(H-C≡) at 3330 cm^{-1} and ν(-C≡CH) at 685 cm^{-1} were also observed over catalysts of Ag on alumina based supports, Ag/Ca and Ag/RX3, respectively. These interactions are predominant over catalysts with Ag active sites, and can be attributed to different electronic species.

In **Figure 7** are shown the *in situ* DRIFTS studies during 1-Pentyne hydrogenation over Ag catalysts at 5 and 15 min of reaction time**.** The DRIFTS peaks of alkyne on the catalysts surface show significant characteristic vibrations peaks of 1-Pentyne with different intensities. Furthermore, characteristic ν(-C=C-) vibrations of 1-Pentene are observed at 1700-1640 cm^{-1}, while ν(C-H) vibrations of vinyl groups can be seen at 3100-3000, 1450-1400 and 1000-900 cm^{-1} over the catalysts during *in situ* DRIFTS hydrogenation [16, 29, 30, 33, 47]. The highest adsorptions of the alkene is observed over Ag/Al and Ag/AlMg catalysts. Over Ag/Al, are observed ν(H-C=) vibrations of 1-Pentene at 3080, 965 and 830 cm^{-1}, and ν(-C=C-) at 1710 cm^{-1}. While, peaks of di-π ν(-C≡C-) bonds at 1519, 1346 cm^{-1} and di-σ ν(-C=C-) bonds at 1615, 1260 cm^{-1} with quite similar intensity are also observed. On the other hand, for Ag/AlMg vibrations of ν(H-C=) at 3065, 1087 and 889 cm^{-1} and ν(-C=C-) at 1721 cm^{-1} attributed to 1-Pentene, are observed; while the band di-π of ν(-C≡C-) bond of the alkyne at 1450 cm^{-1} is more intense than other catalysts. While, peaks of di-σ ν(-C=C-) bond at 1600 and 1250 cm^{-1} show less intensities. The high adsorption, previously discussed is attributed to electron donation from adsorbed species to the ***d*** metal orbitals of the Ag particles supported over Al or AlMg. These catalysts had the best measured properties (high dispersion for the superficial atomic ratios, low particle sizes and high acidity) for the electronic influence of these supports. These results indicate a high dissociative chemisorption of alkyne over these catalysts, which could promote the hydrogenation reaction. On the other hand, for Ag supported on Al and AlMg intermediate species between OH groups and 1-Pentyne also are observed, indicating which type of superficial OH groups participate during the hydrogenation reaction. On Ag/Ca and Ag/RX3 catalysts, less adsorption of intermediate species is observed during *in situ* DRIFTS hydrogenation as vibrations of ν(H-C=) species of 1-Pentene at 3068, 1082 cm^{-1} and 3040, 1089, 928 cm^{-1} are observed, respectively. ν(-C=C-) vibrations characteristic of 1-Pentene are not observed between 1700-1640 cm^{-1} in comparison to Ag/Al and Ag/AlMg. The spectrum of Ag/Ca show peaks of species adsorbed on $Ca^{+2}CO_3^{-2}$, being the peak at 3337 cm^{-1} the most intense. Furthermore, it is observed di-σ ν(-C=C-) bond species at 1260 cm^{-1} with higher intensity in comparison to the evaluated catalysts. The high presence of species at 3337 cm^{-1} ν(H-C≡) for Ag/Ca is attributed to the basic character of the catalyst or the support. In this catalyst the 1-Pentyne can interact mainly because its hydrogen bond is remarkably acidic, due to the high *s* characteristic of the *sp* C-H bond [49]. Due to this acidity, the terminal alkyne hydrogen dissociates upon interaction with a sufficiently strong base. The terminal alkyne then becomes a

carbanion that can serve as a nucleophile in subsequent reactions, in this case could promote the hydrogenation reaction [50].

Over Ag/RX3 di-π ν(-C≡C-) and di-σ ν(-C=C-) bonds species are observed at 1465 cm^{-1} and 1260 cm^{-1}, respectively. The last peak is more intense in this region 1500 - 1200 cm^{-1}. Besides, the greatest intensity of the peak continues to be observed at 650 cm^{-1} due to ν(-C≡CH) bonds; the presence of these bands could indicate a high concentration of 1-Pentyne species over functional groups of RX3 activated carbon.

The peaks evidenced over Ag/Ca and Ag/RX3 at 3337 and 650 could be considered as hydrocarbon species with the role of spectators or related species to the growth process of oligomers formations during the hydrogenation processes [29, 33, 45, 47].

The previous analysis shows that there are different interactions of the adsorbed substrate over each catalyst; as observed with the adsorbed intermediate species formed during the hydrogenation reaction.

Selective Hydrogenation of 1-Pentyne and Olefin Purification

The selective hydrogenation of pure 1-Pentyne, **test 1** and the purification of 1-Pentene of an alkene/alkyne mixture (70:30 % vol), **test 2** were selected as model reactions to evaluate the performance and catalytic properties of the synthesized Ag catalysts.

Figure 8 (a) shows the results of total conversion of 1-pentyne (*X*) as a function of time and **Figure 8 (b)** shows the selectivity to 1-pentene (*S*) as a function of total conversion during the hydrogenation of pure 1-pentyne. The results show that all the catalysts are active and selective to 1-pentene. The observed order of total conversion is: AgAl/ > Ag/Al-Mg > Ag/RX3 > Ag/Ca. For Ag/Ca catalyst it can be observed a very low conversion of 1-pentyne up to 60 min, possible an inductive period of time is necessary, but after this time the reaction rate considerably increased. Ag/Al and Ag/Al-Mg catalysts presented very high selectivities to 1-pentene ≥ 89 %, while for Ag/Ca and Ag/RX3, high selectivity, ca. 81 % are observed.

Table 3 contains values of the initial reaction rates (r^0), the turnover frequency (TOF) and selectivity at isoconversion conditions (X≈99.9 %) during the 1-pentyne hydrogenation reaction (**test 1**). The following order of r^0 is observed during the hydrogenation of pure 1-pentyne: Ag/AlMg ≥ Ag/Al > Ag/RX3 >>Ag/Ca.

According to the very high initial reaction rates and selectivity to the desired product, a good synergism is obtained between the Ag nanoparticles species and the alumina based supports. On the other hand, Ag/RX3 showed high activity and selectivity, while Ag/Ca had the lowest initial reaction rate and high selectivity.

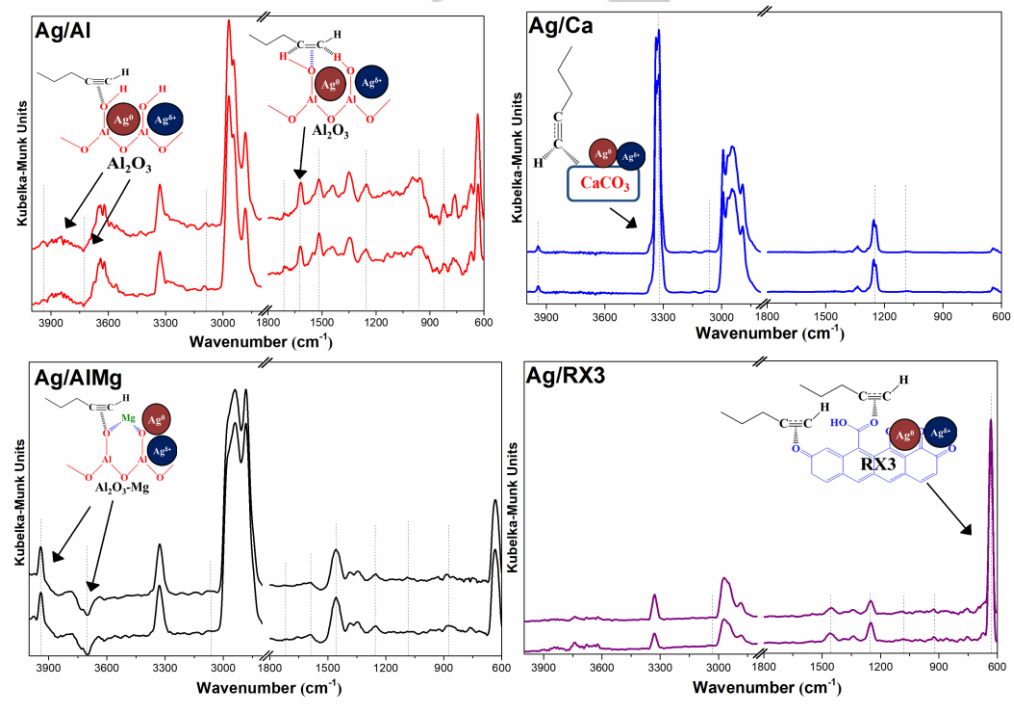

Figure 7. In situ DRIFTS analysis during 1-Pentyne hydrogenation over synthetized catalysts at 5 and 15 min.

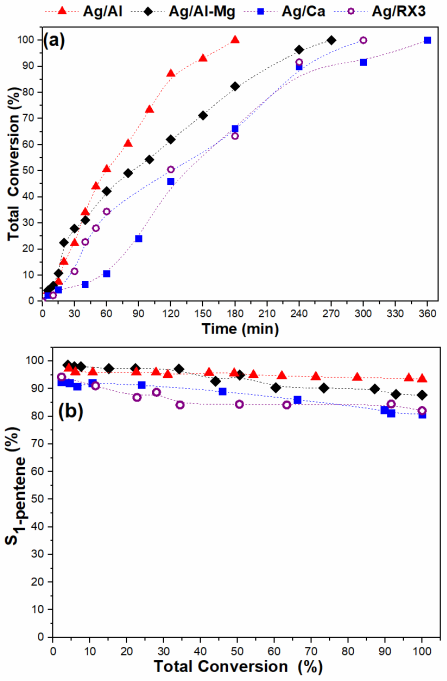

Figure 8. (a) Total Conversion of 1-Pentyne (%) vs. Time (min) and (b) Selectivity to 1-Pentene (%) vs. Total Conversion (%) for Ag/Al (▲), Ag/AlMg (♦), Ag/Ca (■) and Ag/RX3 (○).

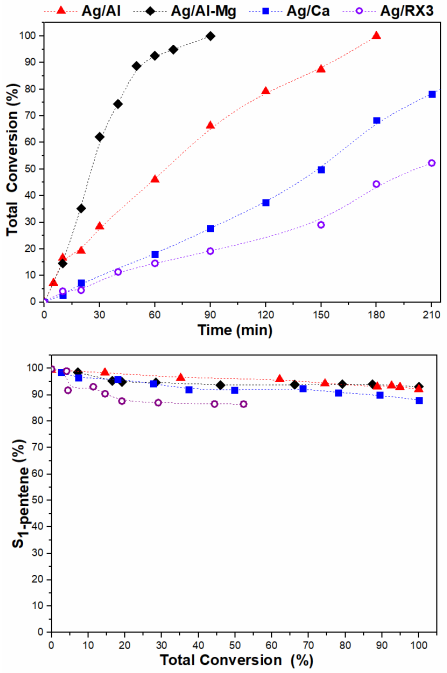

Figure 9. (a) Total Conversion of 1-Pentyne (%) vs. Time (min) and (b) Selectivity to 1-Pentene (%) vs. Total Conversion (%) during the hydrogenation of the 1-pentene/1-pentyne mixture (70/30 vol%) for Ag/Al (▲), Ag/AlMg (♦), Ag/Ca (■) and Ag/RX3 (○).

Figure 9 (a) shows the results of total conversion of 1-pentyne (*X*) as a function of time and **Figure 9 (b)** shows the selectivity to 1-pentene (*S*) as a function of total conversion during the hydrogenation of the 1-pentene/1-pentyne mixture (70/30 vol%). It is observed that the order of activity found is: Ag/Al-Mg >> Ag/Al >> Ag/Ca >> Ag/RX3. All the synthesized catalysts present very high selectivity to 1-pentene: ≥ 90%.

Table 3 contains values of the initial reaction rate (r^0) and selectivity at isoconversion conditions (X≈99.9 %) for the 1-pentene/1-pentyne mixture, 70/30 vol % (**test 2).** The following order of r^0 was observed during the hydrogenation of pure 1-pentyne: Ag/AlMg >> Ag/Al >> Ag/Ca > Ag/RX3.

The Ag/AlMg and Ag/Al catalysts showed the highest r^0 values when evaluated in the 1-pentyne hydrogenation of the 1-Pentene/1-Pentyne mixture of 70/30 vol% (**test 2**), even at shorter times compared to the hydrogenation of the pure alkyne (**test 1**) with high selectivities (≥ 90%). Besides, Ag/Ca and Ag/RX3 catalysts, presented lower values of r^0 with very good selectivity (≥ 86%) up to 210 min of reaction time (**Figure 9, b**). Furthermore, over Ag/Ca the initial reaction rate is 5.1 times higher when the purification is evaluated, while r^0 of Ag/RX3 is identical in both conditions. Besides, during the purification of 1-pentene with the Ag/supported catalysts high selectivity to 1-pentene without marked over-hydrogenation or isomerization processes despite the higher concentration of alkene in the mixture.

The TOF values for 1-pentyne hydrogenation and purification of 1-pentene/1-pentyne mixture present values between 0.20-0.65 and 0.44-1.27 min^{-1}, respectively. The synthesized catalysts showed lower TOF values during the 1-pentyne hydrogenation, than those obtained during the purification of 1-pentene/1-pentyne(70/30 vol%) mixture. The different values of TOF could be attributed to electronic effects.

Previously published works of our group related to the activity and selectivity of monometallic Pd catalysts [7, 11], showed greater activities with respect to Ag catalysts were observed. In fact, the Ag catalysts evaluated showed higher selectivity values compared to that obtained with the monometallic Pd/supported and commercial Lindlar catalysts.

Table 3. Comparison of initial reaction rates (r^0), turnover frequency (TOF) and selectivity to 1-pentene (S) at isoconversion conditions during 1-pentyne hydrogenation (test 1) or purification of 1-pentene/1-pentyne mixture (70/30 vol%, test 2).

Catalysts	Test	t (min)	*X* (%)	S (%)	r^0 (mol $g_{Ag}^{-1}min^{-1}$)	TOF (min^{-1})
Ag/Al	1	180	99.9	88.7	7.2	0.20
Ag/AlMg		270	99.9	93.5	7.5	0.22
Ag/Ca		360	99.9	80.8	1.4	0.25
Ag/RX3		300	99.9	82.3	6.9	0.65
Ag/Al	2	180	99.9	93.1	16.5	0.44
Ag/AlMg		90	99.9	92.1	34.2	1.00
Ag/Ca		270	99.9	88.0	7.2	1.27
Ag/RX3		210	52.3	86.5	6.8	0.64

For Ag/AlMg similar values of r^0 were observed compared to the commercial Lindlar catalyst (36 mol $g_{pd}^{-1}min^{-1}$) during the hydrogenation of 1-pentyne in the mixture of 70:30 vol% indicating a comparable initial activity with very high selectivity to 1-pentene formation [7, 11].

The physicochemical properties and catalytic performance of the Ag/Supported catalysts show that they promote the dissociative adsorption of hydrogen, indicating that the hydrogenation process can be generated over these species. Bibliographic reports and the use of Ag species as catalytic promoters show that Ag

particles have less reactivity towards H_2 dissociation [51, 52]. Dihydrogen dissociation over Ag sites presents high activation barriers even with low surface coordination of the sites, therefore several authors have proposed different mechanisms to the traditional dissociative adsorption of H_2 [17]. For example, Yang *et al*. evidenced that selective hydrogenation of acetylene over Cu(211), Ag(211) and Au(211) can follow Horiuti–Polanyi mechanism or non-Horiuti–Polanyi mechanisms [53]. From this, Ag/SiO_2 [22, 54], Ag/TiO_2 [54, 55] or other catalysts have been used for the selective hydrogenation of alkynes given the best selectivity results offered by these catalysts [18, 20, 23, 56].

Figure 10 shows the proposed interaction of Ag species (Ag^0 / $Ag^{\delta+}$) with supports during selective hydrogenation and olefin purification. The results are related to the intermediate species observed by in situ DRIFT and to the electronic and geometric effects of the catalysts.

i. Ag/AlMg and Ag/Al evaluated catalysts showed the highest r^0 and selectivity values, indicating a great synergistic effect and strong metal-support interaction (SMSI) between the Ag particles with the Al_2O_3 and Al_2O_3–Mg supports. Electronic effects were originated by more accesible NPs of Ag^0 and $Ag^{\delta+}$ sites (rich in d^{10} electrons) for electron donation from Al_2O_3 and Al_2O_3–Mg supports to Ag. The presence of smallest particles size of Ag^0 and $Ag^{\delta+}$, promoting the dissociative adsorption of H_2 for the hydrogenation reaction. Besides, the properties of supports and intermediate adsorbed species (observed by *in situ* DRIFTS) favor the adsorption and desorption of alkyne, 1-pentyne intermediate species and alkene.

ii. Ag/Ca y Ag/RX3 have a less synergistic effect and weak metal-support interaction (WMSI) between the Ag particles with the $CaCO_3$ and RX3 supports. Electronic effects were originated by electron donation from Ag to $CaCO_3$ and RX3 supports. The presence NPs of Ag with highest and intermediate particle sizes (geometric effects) decrease the dissociative adsorption rate of H_2 for the hydrogenation reaction; as a consequence, these catalysts show the lowest activity. Besides, less adsorption of alkyne/alkene intermediate species were observed during *in situ* DRIFTS hydrogenation studies (electronic effects), being this factor the main responsible of the low activity of these catalysts.

Taking into account the above results, on the basis of its high activity and selectivity (>90 %), the best catalysts for the purification of alkenes and/or the hydrogenation of pure terminal alkynes are Ag/AlMg and Ag/Al.

Conclusions

Ag nanoparticles were synthesized over four different supports: γ-Al_2O_3, γ-Al_2O_3 modified with Mg, $CaCO_3$ and activated carbon RX3.

As observed by XPS, TEM, XRD and ICP studies, the nanoparticle size, dispersion and the superficial species, suggest the influence of both electronic and geometric properties. Metal-support interaction (MSI) have the greatest influence on the selective hydrogenation reactions evaluated, especially superficial groups over the support favors the adsorption of the alkyne, and the more accesible Ag sites (d^{10}) that promote the dissociative adsorption of hydrogen. Besides, the small particle size favor the hydrogenation rate of the catalysts. In this context, the evaluated Ag/AlMg and Ag/Al catalysts showed a great synergistic effect and strong metal-support interaction (SMSI) with lowest particle size. While Ag/Ca and Ag/RX3 have a less synergistic effect and weak metal-support interaction (WMSI) with highest and medium particle size.

By *in situ* DRIFT studies, Ag/AlMg and Ag/Al showed the highest amount of intermediate adsorbed species of 1-pentyne and 1-pentene, these could be responsible of increasing the hydrogenation reaction rate and the high selectivity. While over Ag/Ca and Ag/RX3, high interaccions intermediate species were observed, responsible of less catalytic activity of both catalysts.

Selective hydrogenation of 1-pentyne and purification of 1-pentene from the olefinic stream (1-pentene/1-pentyne, 70/30 vol %) was achieved. From these results a preferential hydrogenation of C≡C in the mixtures was observed, indicating that the alkyne has the greatest tendency to be the first to be reduced. The Ag catalysts supported on Al_2O_3-Mg and Al_2O_3 presented the highest values of activity and selectivity to the desired product ~ 90-94%. Metal-support interactions, geometric and electronic properties during the hydrogenation reactions, have the major influence of the adsorbed intermediate species responsible of the catalytic performance.

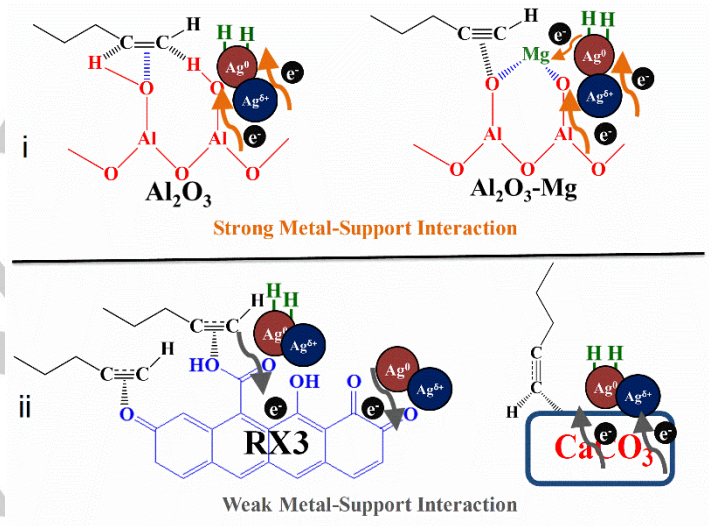

Figure 10. Proposed interaction of Ag species with supports during selective hydrogenation and olefin purification.

Acknowledgments

The economic supports of ANPCyT, UNL and CONICET are appreciated.

Keywords: In situ DRIFTS, Alkynes, Alkyne/Alkene, Selectivity, Silver, Supports

Experimental Section

Catalyst Preparation

Four materials of different acidity and physical properties were used as support in this study: $CaCO_3$ (Anedra, purity 98.6%), NORIT® RX3 EXTRA activated carbon (acid-washed, steam-activated carbon) and γ-Al_2O_3 (CK-300 powdered, mesh 35-80, previously calcined 3 h at 823 K). NORIT® RX3 EXTRA and $CaCO_3$ were used without previous treatment. A fraction of alumina was treated with an aqueous solution of $MgSO_4.7H_2O$ (Anedra, purity 99.8 %) in order to obtain ca. 5 wt % of Mg: then was dried 24 h at 373 K and calcined for 3 h at 823 K. Alumina solids were called Al_2O_3 and Al_2O_3-Mg, respectively.

Supported Ag catalysts were obtained by incipient wetness technique. The impregnation was performed using solution of $AgNO_3$ (Aldrich, purity 99.0 %) at pH= 1 for alumina or carbon supports, while pH=5 was used for $CaCO_3$ support. The solutions were stirred and sonicated during 20 min at 42 kHz and 100W (using a Branson Ultrasonics 2510 equipment). Then, the synthetized catalysts were dried at 393 K during 24 h. Samples on Al_2O_3 and Al_2O_3-Mg were calcined in air at 823 K for 3 h; while the samples on $CaCO_3$ and RX3 were pretreated with a N_2 flow during 3 h at 823 K in order to stabilize metallic nanoparticles, and avoid the support decomposition in an inert atmosphere. Finally, all the catalysts were reduced 1 h at 673 K in a H_2 stream at 50 mL min^{-1} in a tubular continuous flow quartz reactor. The theorical charge on the catalyst was ca. 0.5 wt % of Ag. The catalysts were identified: Ag/Al, Ag/Al-Mg, Ag/Ca, and Ag/RX3.

Catalysts Characterization

A Micromeritics ASAP 2020 instrument was used to obtain the nitrogen adsorption-desorption isotherms between 0.02 and 0.98 relative pressures (P/P_o) and the Brunauer–Emmett–Teller (BET) model was used to calculate the specific surface area (S_{BET}) of the supports. Samples were outgassed 2 h at 523 K under vacuum, and then N_2 adsorption isotherms at 77 K were obtained.

The mass content of Ag in the catalysts was determined by Atomic Emission Spectroscopy with Inductive Plasma (ICP-OES) using a Perkin Elmer OPTIMA 2120 equipment, after digestion of the samples in diluted sulfuric acid solution at 363 K.

The electronic state of surface species and their superficial atomic relationships were obtained by X-Ray Photoelectron Spectroscopy (XPS), following the Pd $3d_{5/2}$, Ca $2p_{3/2}$, and 2p peak position of Mg, Cl and Al. The measurements were made on a VG-Microtech Multilab instrument equipped MgK_α (hυ: 1253.6 eV) and an energy flow of 50 eV. The analysis pressure during data acquisition was maintained at 5.10^{-7} Pa. The samples were previously reduced 1 h at 673 K in H_2 flow, following the same pretreatment conditions, previous to the catalytic evaluation. The areas of the peaks were estimated by calculating the integral of each peak after subtracting a Shirley background and fitting the experimental peak to a combination of Lorentzian/Gaussian lines of 30–70% proportions. The binding energy used as reference were the Al 2p at 74.7 eV, Ca $2p_{3/2}$ at 346.6 eV and C 2p at 284.6 eV, respectively for the Al_2O_3, $CaCO_3$ and C supports.

The crystalline structure of the catalysts was defined in an X-ray Diffraction (XRD) Shimadzu XD-D1 equipment, with a CuK_α (λ = 1.5405 Å) in the range $10 < 2\theta < 85^o$, at 1^o min^{-1} scanning speed. Powdered samples were reduced *ex situ* in H_2 stream.

The metal particle size distribution was obtained by TEM using a JEOL-2100 Plus electron microscope with an acceleration voltage of 200 kV and HRTEM mode. The samples were prepared by grinding the pellets, suspending the particles in ethanol and then sonicating for 15 min. A drop of this suspension was placed on a 200 mesh copper grid with a Formvar film and observed. A set of digital images were taken in order to identify the phases and measure the particle diameters. Digital Micrograph software was used to obtain the particle size distributions.

In situ DRIFTS Studies

In situ DRIFTS (Diffuse Reflectance Infrared Spectroscopy) analysis was performed in a Shimadzu Affinity-1S FTIR equipment, coupled to a DRIFTS thermal cell with a ZnSe mirror. For each analysis ~ 30 mg of catalyst was reduced *in situ* 30 min in H_2 flow at 673 K then subjected to vacuum and cooled down up to 303 K. The background of the samples was recorded and the adsorption experiments were carried out, passing through the saturator 5 mL min^{-1} of N_2 or H_2 with 200 µL of pure 1-pentyne at 303 K and 1 atm, equivalent to 0.015 molar fraction of alkyne. The analysis was performed every 2 min during 30 min in transmittance mode with a resolution of 4 cm^{-1} and 64 scans. The spectra were processed using the Kubelka-Munk method.

Catalytic tests

The catalysts were evaluated during the selective hydrogenation of pure 1-pentyne (Aldrich, Cat. No. 627-19-0, purity > 99%) or the purification of a mixture of 1-pentene (Aldrich, Cat. No. 109-67-1, > 98.5%) /1-pentyne (70/30 vol %). The operational conditions used were: 1.5 atm, 303 K, and a molar ratio of substrate/Pd = 1100 (S/Pd). 50 mL of a solution of 2 vol % of substrate in toluene (Merck, Cat. No. TX0735-44, > 99%). A stainless steel batch reactor coated with polytetrafluoroethylene (PTFE) was used during the catalytic tests. An agitation speed of 750 rpm was used in order to eliminate external diffusional limitations. The reagents and products were analyzed by gas chromatography (GC) with an FID detector and HP INNOWax capillary column of Polyethyleneglycol (PEG).

References

[1] L. Zhang, M. Zhou, A. Wang, T. Zhang, *Chem. Rev.* **2020**, 120, 683-733.

[2] G. Vilé, D. Albani, N. Almora-Barrios, N. López, J. Pérez-Ramírez, *ChemCatChem*. **2016**, 8, 21-33.

[3] X. Zhao, Y. Chang, W.-J. Chen, Q. Wu, X. Pan, K. Chen, B. Weng, *ACS Omega*. **2022**, 717-31.

[4] L.B. Belykh, N.I. Skripov, T.P. Sterenchuk, T.A. Kornaukhova, E.A. Milenkaya, F.K. Schmidt, *Mol.Catal.* **2022**, 528 112509.

[5] D. Zhao, X. Liu, D. Wang, X. Zhou, Z. Liu, W. Yuan, *J. Cleaner Prod*. **2019**, 220, 289-297.

[6] A. Jung, A. Jess, T. Schubert, W. Schütz, *Appl. Catal., A*. **2009**, 362 95-105.

[7] M. Cordoba, C. Betti, L. Martínez Bovier, L. García, F. Coloma-Pascual, A. Ramírez, M.E. Quiroga, C.R. Lederhos, *J. Chem. Technol. Biotechnol*. **2021**, 96, 2283-2297.

[8] A.J. McCue, A. Guerrero-Ruiz, C. Ramirez-Barria, I. Rodríguez-Ramos, J.A. Anderson, *J. Catal*. **2017**, 355, 40-52.

[9] M. Eggersdorfer, D. Laudert, U. Létinois, T. McClymont, J. Medlock, T. Netscher, W. Bonrath, *Angew. Chem., Int. Ed*. **2012**, 51, 12960-12990.

[10] L.Z. Nikoshvili, A.S. Makarova, N.A. Lyubimova, A.V. Bykov, A.I. Sidorov, I.Y. Tyamina, V.G. Matveeva, E.M. Sulman, *Catal. Today*. **2015**, 256 ,231-240.

[11] M. Cordoba, F. Coloma-Pascual, M.E. Quiroga, C.R. Lederhos, *Ind. Eng. Chem. Res*. **2019**, 58, 17182-17194.

[12] B. Bridier, N. López, J. Pérez-Ramírez, *J. Catal*. **2010**, 269, 80-92.

[13] F. Unglaube, C.R. Kreyenschulte, E. Mejía, *ChemCatChem.* **2021**,13, 2583-2591.

[14] Y. Song, S. Weng, F. Xue, A.J. McCue, L. Zheng, Y. He, J. Feng, Y. Liu, D. Li, *ACS Catal*. **2023**, 13 1952-1963.

[15] M. Armbrüster, K. Kovnir, M. Friedrich, D. Teschner, G. Wowsnick, M. Hahne, P. Gille, L. Szentmiklósi, M. Feuerbacher, M. Heggen, F. Girgsdies, D. Rosenthal, R. Schlögl, Y. Grin, *Nat. Mater.* **2012**, 11, 690-693.

[16] Z. Li, J. Zhang, J. Tian, K. Feng, Z. Jiang, B. Yan, *Chem. Eng. J*. **2022**, 450, 138244.

[17] G. Vilé, D. Baudouin, I.N. Remediakis, C. Copéret, N. López, J. Pérez-Ramírez, *ChemCatChem*. **2013** 5, 3750-3759.

[18] R. Chanerika, M.L. Shozi, H.B. Friedrich, *ACS Omega*. **2022**, 7, 4026-4040.
[19] X.-Y. Dong, Z.-W. Gao, K.-F. Yang, W.-Q. Zhang, L.-W. Xu, *Catal. Sci.* Technol. **2015** , 5, 2554-2574.
[20] G. Fang, X. Bi, *Chem. Soc. Rev*. **2015**, 44, 8124-8173.
[21] F. Cárdenas-Lizana, Z.M.D. Pedro, S. Gómez-Quero, L. Kiwi-Minsker, M.A. Keane, *J. Mol. Catal. A: Chem.* **2015**, 408, 138-146.
[22] E. Oakton, G. Vilé, D. S. Levine, E. Zocher, D. Baudouin, J. Pérez-Ramírez, C. Copéret, *Dalton Trans.* **2014**, 43, 15138-15142.
[23] C. Wen, A. Yin, W.-L. Dai, *Appl. Catal., B*. **2014**, 160-161, 730-741.
[24] O.V. Vodyankina, G.V. Mamontov, V.V. Dutov, T.S. Kharlamova, M.A. Salaev, *Adv. Nanomater. Catal. Energy*, **2019**, 143-175.
[25] C.-J. Pan, M.-C. Tsai, W.-N. Su, J. Rick, N.G. Akalework, A.K. Agegnehu, S.-Y. Cheng, B.-J. Hwang, *J. Taiwan Inst. Chem. Eng.* **2017**, 74, 154-186.
[26] G.-M. Schwab, *Electronics of Supported Catalysts*, in: D.D. Eley, H. Pines, P.B. Weisz (Eds.) Adv.Catal. Academic Press, **1979**, p. 1-22.
[27] M. Crespo-Quesada, F. Cárdenas-Lizana, A.-L. Dessimoz, L. Kiwi-Minsker, Modern Trends in Catalyst and Process Design for Alkyne Hydrogenations, *ACS Catal*. **2012**, 2, 1773-1786.
[28] F. Zaera, *Chem. Soc. Rev*. **2014**, 43, 7624-7663.
[29] M. Cordoba, L. Garcia, L. Martinez Bovier, J. Badano, C. Betti, F. Coloma Pascual, M. Quiroga, C. Lederhos, *Top. Catal*. **2022**, 65, 1347-1360.
[30] J. Wood, M.J. Alldrick, J.M. Winterbottom, E.H. Stitt, S. Bailey, *Catal. Today.* **2007**, 128, 52-62.
[31] R. Henry, M. Komurcu, Y. Ganjkhanlou, R.Y. Brogaard, L. Lu, K.-J. Jens, G. Berlier, U. Olsbye, *Catal. Today.* **2018**, 299154-163.
[32] J. Moon, Y. Cheng, L.L. Daemen, M. Li, F. Polo-Garzon, A.J. Ramirez-Cuesta, Z. Wu, *ACS Catal.* **2020**, 10, 5278-5287.
[33] S. Moussa, P. Concepción, M.A. Arribas, A. Martínez, *ACS Catal*. **2018**, 8, 3903-3912.
[34] S. Vorakitkanvasin, W. Phongsawat, K. Suriye, P. Praserthdam, J. Panpranot, *RSC Adv.* **2017**, 7, 38659-38665.
[35] R.J. Matyi, L.H. Schwartz, J.B. Butt,*Catal. Rev.* **1987**, 29, 41-99.
[36] X-ray photoelectron spectroscopy database NIST standard reference database 20, Version 3.5 (Web version). in, National Institute of Standards and Technology, Gaithersburg, 2007.
[37] J.F. Moulder, J. Chastain, *Handbook of X-ray Photoelectron Spectroscopy: A Reference Book of Standard Spectra for Identification and Interpretation of XPS Data*, Physical Electronics Division, Perkin-Elmer Corporation, 1992.
[38] J. Feng, D. Fan, Q. Wang, L. Ma, W. Wei, J. Xie, J. Zhu, *Colloids Surf., A*, **2017**, 520, 743-756.
[39] A.M. Ferraria, A.P. Carapeto, A.M. Botelho do Rego, *Vacuum*. **2012**, 86, 1988-1991.
[40] Y.H. Kim, D.K. Lee, Y.S. Kang, *Colloids Surf., A*. **2005**, 257-258, 273-276.
[41] L. Gharibshahi, E. Saion, E. Gharibshahi, A.H. Shaari, K.A. Matori, *Materials*. **2017**, 10, 402.
[42] K. Anandalakshmi, J. Venugobal, V. Ramasamy, *Appl. Nanosci*. **2016**, 6, 399-408.
[43] K.R. Jennings, *Spectrometric identification of organic compounds* (Fifth Edition) R. M. SILVERSTEIN, G. C. BASSLER AND T. C. MORRILL. Wiley, New York, 1991.
[44] A. Horn, H. Hopf, P. Klaeboe, *J.Mol. Struct.* **2011**, 989, 38-44.
[45] J. Liu, M.B. Uhlman, M.M. Montemore, A. Trimpalis, G. Giannakakis, J. Shan, S. Cao, R.T. Hannagan, E.C.H. Sykes, M. Flytzani-Stephanopoulos, I, *ACS Catal*. **2019,** 9, 8757-8765.
[46] A.V. Ivanov, A.E. Koklin, E.B. Uvarova, L.M. Kustov, *Phys. Chem. Chem. Phys.* **2003**, 5, 4718-4723.
[47] T. Cao, R. You, X. Zhang, S. Chen, D. Li, Z. Zhang, W. Huang, *Phys. Chem. Chem. Phys.* ***2018***, 20, 9659-9670.
[48] G. Vilé, B. Bridier, J. Wichert, J. Pérez-Ramírez, *Angew. Chem., Int. Ed*. **2012**, 5, 8620-8623.
[49] E. Stauffer, J.A. Dolan, R. Newman, *CHAPTER 3 - Review of Basic Organic Chemistry*, in: E. Stauffer, J.A. Dolan, R. Newman (Eds.) Fire Debris Analysis, Academic Press, Burlington, 2008, pp. 49-83.
[50] F. Diederich, P.J. Stang, R.R. Tykwinski, *Acetylene Chem.* Chemistry, Biology and Material Science, Wiley, 2006.
[51] A.B. Mohammad, K. Hwa Lim, I.V. Yudanov, K.M. Neyman, N. Rösch, *Phys. Chem. Chem. Phys.* ***2007,*** 9, 1247-1254.
[52] A. Montoya, A. Schlunke, B.S. Haynes, *J. Phys. Chem.* ***2006,*** 10, 17145-17154.
[53] B. Yang, R. Burch, C. Hardacre, P. Hu, P. Hughes, *Catal.Sci.Technol*. **2017**, 7, 508-1514.
[54] A. Sárkány, Z. Révay, *Appl. Catal., A*. **2003**, 243, 347-355.
[55] Y.N. Liu, J.T. Feng, Y.F. He, J.H. Sun, D.Q. Li, *Catal.Sci.Technol*. **2015,** 5, 1231-1240.
[56] R. Chanerika, M.L. Shozi, M. Prato, H.B. Friedrich, *Mol. Catal.* **2002,** 525, 112344.

10.1002/cplu.202300344

WILEY-VCH

RESEARCH ARTICLE

Table of Contents

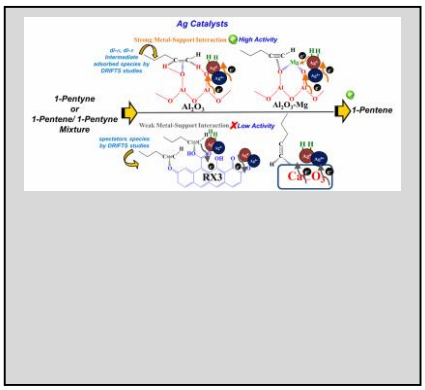

Different -C≡C- and -C=C- adsorbed species were observed on the supports and catalysts surface using *in situ* DRIFT analysis: The species are responsible of the activity and high selectivity during the hydrogenation reaction. The role of the supports and electronic properties of Ag nanoparticles improve the H_2 dissociative chemisorption; promoting the high selectivity and the catalytic performance.

.